

## Corrosion Kinetics of Mild Steel Coated with Titanium-Based Anti-corrosion Polyethylene Wax from Waste LDPE Water Sachets in Brine and Acidic Media

Ejimofo Marcel Ikenna<sup>1\*</sup>, Okey-Onyesolu Faith Chinonye<sup>1\*</sup>, Okeke Winifred Chinelo<sup>2\*</sup>,  
Chinyere Blessing Frank<sup>1</sup>, Ajali John-Jones<sup>1</sup>

<sup>1</sup>Chemical Engineering Department, Nnamdi Azikiwe University, Awka

<sup>2</sup>Chemistry Education Department, Federal College of Education (Technical), Umuze.

\*Corresponding Author's E-mail: [mi.ejimofo@unizik.edu.ng](mailto:mi.ejimofo@unizik.edu.ng), [cf.onyesolu@unizik.edu.ng](mailto:cf.onyesolu@unizik.edu.ng)

---

### Abstract

Corrosion of carbon steel remains a major global challenge across multiple industrial sectors, necessitating efficient and sustainable mitigation strategies. This study presents a novel titanium-based anticorrosion polyethylene wax (TAC-PEW) coating synthesized from discarded low-density polyethylene (LDPE) sachets sourced from sachet water industries. LDPE was pyrolyzed under optimal conditions of 450 °C for 35 min, yielding 60.77 % wax, which was subsequently blended with titanium and other additives to produce TAC-PEW. In acidic media, TAC-PEW provided substantial protection for mild steel with highest inhibition efficiency of 85.7 %. Kinetic analysis showed that the data fitted an exponential decay model with an exceptional correlation coefficient ( $R^2 = 0.9999$ ) and a decay constant of 0.2529 hr<sup>-1</sup>, indicating rapid suppression of the initial corrosion rate. TAC-PEW demonstrates dual environmental and industrial benefits by repurposing non-biodegradable plastic waste into a high-performance, sustainable coating for corrosion control in aggressive environments.

**Keywords:** TAC-PEW, Corrosion, Mild Steel, Inhibition, Kinetics

---

### 1. Introduction

Corrosion of carbon steel is a pervasive problem in numerous industries such as oil and gas, automotive, marine and ship building, manufacturing and industrial sectors, aerospace, among others, leading to substantial economic losses and safety concerns (Aljibori et al., 2024; Al-Amiery et al., 2024; Aljibori et al., 2023). Hence, the problem of carbon steel corrosion is a major challenge that cuts across many sectors. Mitigating corrosion-related issues requires the development of effective and sustainable protective coatings among other inhibitors (Al-Amiery et al., 2024). In recent years, there has been growing interest in utilizing waste materials for the production of innovative anticorrosion coatings (Thomas et al., 2022). This research paper focuses on investigating the application of a novel titanium-based anticorrosion polyethylene wax, derived from waste low-density polyethylene water sachets, for the protection of carbon steel substrates in aggressive environments such as brine and acidic media.

The development of advanced coatings with enhanced corrosion resistance properties is a complex task, requiring a deep understanding of the underlying corrosion kinetics (Thomas et al., 2022). Traditionally, experimental methods have been employed to assess corrosion behavior. However, these approaches can be time-consuming, resource-intensive, and limited in capturing the complex interplay of factors affecting corrosion (Al-Amiery et al., 2024). To overcome these limitations, computational modeling techniques have gained attention as valuable tools for analyzing, predicting, and understanding corrosion kinetics (Jia et al., 2022).

This study proposes the application of a Python-based predictive modeling approach to analyze and forecast the corrosion kinetics parameters of carbon steel coated with the novel titanium-based anticorrosion polyethylene wax (TAC-PEW). The computational framework integrates advanced statistical and data-driven algorithms to estimate optimal model parameters and generate model plots (Raschka et al., 2020). This method enables the development of a robust predictive framework for corrosion behavior, offering insights into the effectiveness of the coating in different environments.

The choice of waste low-density polyethylene water sachets as the precursor for the wax used in the formulation of the novel titanium-based polyethylene wax coating is driven by environmental and sustainability considerations. These sachets are a major source of plastic waste, particularly in regions with limited waste management infrastructure (Raschka et al., 2020). By transforming this waste material into a value-added product with anticorrosion properties, two significant challenges—waste management and corrosion protection—will be simultaneously addressed. The objectives of this research work are twofold. Firstly, to investigate the effectiveness of the enhanced titanium-based polyethylene wax coating in inhibiting corrosion of carbon steel in brine and acidic media. This evaluation involves experimental measurements of corrosion parameters, including corrosion rate and weight loss under controlled conditions. Secondly, to develop and apply Python-based computational models to analyze and predict corrosion kinetics based on the experimental data. This modeling approach enables the exploration of complex corrosion behavior patterns, facilitating the optimization of coating parameters for improved performance.

The outcomes of this research have significant implications for the corrosion protection industry. The utilization of waste low-density polyethylene water sachets for producing an enhanced titanium-based polyethylene wax coating not only contributes to waste management efforts but also offers a sustainable and cost-effective solution for corrosion prevention. The application of a Python-based predictive modeling approach provides a valuable tool for the accurate prediction of corrosion kinetics, enabling the development of advanced coating systems tailored to specific environmental conditions. Finally, this research paper explores the application of computational modeling for studying the corrosion kinetics of carbon steel coated with enhanced titanium-based polyethylene wax derived from waste low-density polyethylene water sachets in brine and acidic media. By combining innovative coatings for corrosion prevention with advanced predictive modeling for kinetic analysis, progress in corrosion protection strategies can be achieved, offering more durable and efficient solutions for various industries.

## 2.0 Materials and methods

### 2.1 Materials

The materials used include: Waste low-density polyethylene films (commonly known as pure water sachets (see Fig 1)) locally sourced within Ifite in Awka South Local Government Area (6.2116° N, 7.0714° E) of Anambra State, Nigeria, the mild steel (conforming to ASTM A36 specification (nominal composition: C ≤ 0.26 wt%, Mn 0.60–0.90 wt%, P ≤ 0.04 wt%, S ≤ 0.05 wt%, balance Fe) , titanium-dioxide (powdered form), alkyd resin, isopropyl alcohol, hydrochloric acid, brine, cobalt(II) naphthenate (commonly known as cobalt drier) and mixed dryer ( a mixture of cobalt(II) 2-ethylhexanoate, zirconium(IV) 2-ethylhexanoate and calcium 2-ethylhexanoate), these materials were procured from a dealer at the bridge head market Onitsha, Anambra State, Nigeria.



**Fig 1: Site of low-density polyethylene from sachet water industries**

### 2.1.1 Sample preparation

The sachets from used sachet water were washed and sun dried, thereafter, the sachets were bleached using nitrocellulose to remove ink imprints. The recovered samples were allowed to dry under room temperature and thereafter shredded and set for pyrolysis.

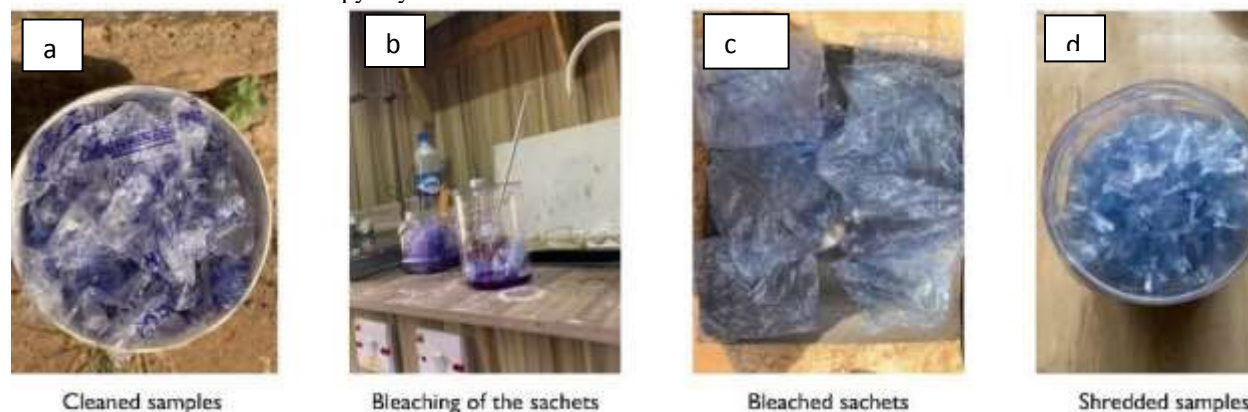


**Fig 2: Sample preparation**

### 2.2 Production of PEW

The pyrolysis experiment was carried out using SX-5-12 WIMCOM scientific muffle furnace.

Pre-weighed shredded sachets samples were introduced into the burning chambers of the muffle furnace. The pyrolysis experiment was conducted at varying temperature (623K and 723K) and residence time of 35 minutes and 60 minutes (Dubdub & Al-Yaari, 2020). After the desired residence time, the resulting polyethylene wax (PEW) was allowed to cool to room temperature, collected and weighed.

The wax yield was estimated using Equation 1:

$$Y_w = \frac{X_2}{X_1} \times 100\% \quad 1$$

where  $Y_w$  is the yield of wax in percentage,  $X_2$  is the mass of the wax obtained from pyrolysis, and  $X_1$  is the initial mass of the samples.

### 2.3 Characterization of PEW

The PEW was analyzed using Cary 630 FTIR spectrometer by Agilent Technology US to observe the functional groups present in PEW. Micrograph Analysis similar to Scanning electron microscopy (SEM) experiments was conducted to identify the physical morphology of the surfaces. The wax hardness was estimated using a durometer (ASTM D2240). The thermo-gravimetric analysis (TGA) on PEW was carried out using a NETZSCH thermo-gravimetric analyzer.



**Fig 3: Polyethylene wax recovered from pyrolysis of waste sachets from sachet water industries**

## 2.4 Solvent Selection for TAC-PEW

The choice of solvent was made between Xylene and isopropyl alcohol (IPA), both of which were used to dissolve the alkyd at ratio 1:1.5 for the solvent and the alkyd. The selection was based on the observed solubility in-terms of viscosity and consistency (Dubdub & Al-Yaari''2020).

## 2.5 Formulation of TAC-PEW

The TAC-PEW was formulated using different ratios of titanium dioxide, xylene, alkyd resin, mixed dryer and cobalt dryer. Varying mass of PEW was melted in a 250ml pyrex beaker using controlled temperature magnetic stirrer at 70 degree temperature. The desired volume of xylene was introduced as solvent and the mixture was allowed to stirrer for 20min. Thereafter, xylene was used as solvent. Different masses of alkyd resin were dissolved in the mixture. Another 20min residence time was allowed to enhance the mixing consistency. Varying weights of titanium dioxide was introduced into the mixing vessel and other additives were added in proportions. Then the mixture was allowed to blend. Samples were analyzed and stored for corrosion inhibition efficiency experiment. Effect of solvent-titanium dioxide-PEW ratio in TAC-PEW coating formulation was evaluated.

## 2.6 Anti-corrosion efficiency experiment of the TAC-PEW coating

Four carbon steel samples were watched and allowed to dry; this was done to remove possible impurities. Thereafter, three of the samples were uniformly coated with the 10 ml of the TAC-PEW coating and were allowed to dry under room temperature for four hours. The one not coated was used as control. The samples were weighed and the initial samples weight recorded (approximately, the samples weight was constant 5.1 for the samples coated with TAC-PEW and 4.81 for the control). Each of the samples was introduced into 50 ml of dilute hydrochloric acid, brine and H<sub>2</sub>O under different temperature conditions (however, for estimating the kinetics, corrosion rate dependence on time at 30°C was used for this study). The samples were reweighed every 1 hr interval and the weight loss estimated. The corrosion rate was calculated using Equation 2

$$CR = \frac{K \cdot m_{loss}}{A \cdot t \cdot \rho} \quad 2$$

where  $k$  is a constant  $8.76 \cdot 10^4$  so that CR is in [mm/y],  $m_{loss}$  is the mass loss [g] of the metal ( $m_0 - m_t$ ) in time  $t$  [hours],  $A$  is the surface area of the material exposed [cm<sup>2</sup>], and  $\rho$  is the density of the material [g/cm<sup>3</sup>] (ASTM, 2012)

## 2.7 Model description

### 2.7.1 Corrosion kinetic models for carbon steel

Corrosion kinetic models are mathematical representations that describe the rate of corrosion for a given material under specific conditions (Enikeev et al.,2020). These models help predict and understand the corrosion behavior of materials, allowing for better corrosion prevention and control. The data were modeled using four different corrosion kinetic models. These models include the linear mode 1(Equation 3, parabolic rate model (Equation 4), exponential rate model (Equation 5) and Logarithmic rate model (Equation 6) (see Table 1).

Table 1: Corrosion kinetics model equations based on corrosion rate

| Model                | Mathematical Description | Constants | Equation No | References          |
|----------------------|--------------------------|-----------|-------------|---------------------|
| Linear Rate Model    | CR = Kt                  | K         | 3           | Enikeev et al.,2020 |
| Parabolic Rate Model | CR = k * √(t)            | K         | 4           | Tian et al.,2024    |
| Exponential Model    | CR = k * exp(-βt)        | k and β   | 5           | Tian et al.,2024    |
| Logarithmic Model    | CR= k * log(t)           | K         | 6           | Tian et al.,2024    |

## 2.8 Inhibition studies

The effectiveness of TAC-PEW in corrosion inhibition was studied using the weight loss of uncoated and coated steel in acidic medium. The inhibition efficiency is a measure of how well the TAC-PEW reduces the corrosion rate compared to the case without the coating. It was expressed as a percentage (Shwetha et al.,2024). The inhibition efficiency (IE) can be calculated using Equation 7

$$IE = \frac{CR_{uc} - CR_c}{CR_{uc}} * 100 \quad 7$$

Where CR<sub>UC</sub> is the corrosion rate of the control sample (uncoated steel), CR<sub>C</sub> = corrosion rate of coated samples.

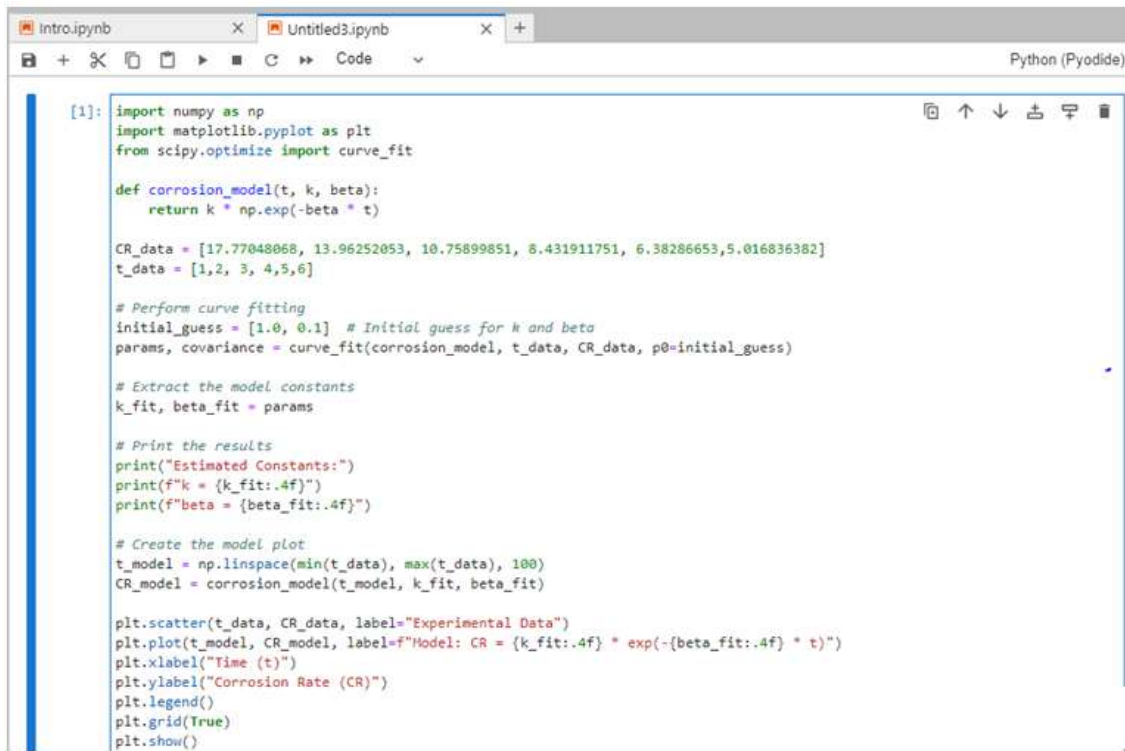
A higher inhibition efficiency value indicates better protection against corrosion by the TAC-PEW. Furthermore, the kinetics of corrosion inhibition was modeled using inhibition equations in Table 2 below.

Table 2: Corrosion inhibition kinetics model equations based on Inhibition efficiency

| Model              | Model Description                      | Equ. No | References                  |
|--------------------|--|---------|-----------------------------|
| Linear Model       | $IE(t) = a + b * t$                    | 8       | Castillo-Robles et al.,2024 |
| Exponential model  | $IE(t) = a * \exp(-b * t)$             | 9       | Castillo-Robles et al.,2024 |
| The logistic model | $IE(t) = a / (1 + \exp(-b * (t - c)))$ | 10      | Castillo-Robles et al.,2024 |
| Power Law Model    | $IE(t) = a * t^b$                      | 11      | Castillo-Robles et al.,2024 |

## 2.9 Python coding sample for kinetic data modeling

The corrosion kinetics models in Table 1 were evaluated in Python using the data fitting, the data fitting techniques were provided by NumPy and SciPy libraries. The Numpy function was used to array the data and specify the model equation, thereafter; the curve fit function from SciPy fitted the data to the model, obtaining the kinetic model's parameters. The models's parameters were used to generate the curve while the data points were plotted along with the model curve using matplotlib. Thereafter CR prediction code were raised for coefficient validation and CR prediction and the correlation coefficient and error function values were evaluated using the experimental data set and the predicted data set. Plate 1 shows the kinetic model coding for the exponential decay corrosion kinetic model as a representative sample. Others coding for the models under consideration (Table 1) are presented as supplementary material. The codes represent a pathway for both the kinetic plot generation and evaluation of the optimal kinetic parameters. Furthermore, another set of codes were raised using the optimized coefficients and constants as data inputs for CR prediction as a means of validation. For the IE kinetics, curve fitting was first carried out using the curvefit function from SciPy to find the optimized coefficients. Thereafter, new sets of IE values were predicted using the fitted coefficients for a range of the set of t values, and then the model plot was raised using both the original data and the fitted curve to obtain the best fit model.



```
[1]: import numpy as np
import matplotlib.pyplot as plt
from scipy.optimize import curve_fit

def corrosion_model(t, k, beta):
    return k * np.exp(-beta * t)

CR_data = [17.77048068, 13.96252053, 10.75899851, 8.431911751, 6.38286653, 5.016836382]
t_data = [1, 2, 3, 4, 5, 6]

# Perform curve fitting
initial_guess = [1.0, 0.1] # Initial guess for k and beta
params, covariance = curve_fit(corrosion_model, t_data, CR_data, p0=initial_guess)

# Extract the model constants
k_fit, beta_fit = params

# Print the results
print("Estimated Constants:")
print(f"k = {k_fit:.4f}")
print(f"beta = {beta_fit:.4f}")

# Create the model plot
t_model = np.linspace(min(t_data), max(t_data), 100)
CR_model = corrosion_model(t_model, k_fit, beta_fit)

plt.scatter(t_data, CR_data, label="Experimental Data")
plt.plot(t_model, CR_model, label=f"Model: CR = {k_fit:.4f} * exp(-{beta_fit:.4f} * t)")
plt.xlabel("Time (t)")
plt.ylabel("Corrosion Rate (CR)")
plt.legend()
plt.grid(True)
plt.show()
```

Plate 1: coding for exponential kinetic model

## 2.10 Model Error analysis

The statistical error functions utilized include the coefficient of correlation, non-linear chi-squared and standard deviation.

$$R^2 = \frac{\sum_{i=1}^n (I_{e.cal} - I_{e.exp})^2}{\sum_{i=1}^n (I_{e.cal} - I_{e.exp})^2 + (I_{e.cal} - I_{e.exp})^2} \quad 12$$

$$Chi\ squared = \sum \frac{(I_{e.exp} - I_{e.cal})^2}{I_{e.exp}} \quad 13$$

$$SD = \sqrt{\frac{1}{(N-1)} \sum_{i=1}^N \left( \frac{I_{e.exp} - I_{e.pred}}{I_{e.exp}} - AARE \right)^2} \quad 14$$

## 3.0 Result and Discussion

### 3.1 Pyrolysis of waste sachets

Waste sachets from sachet water packaging typically consist of low-density polyethylene (LDPE) and other additives such as pigments, stabilizers, and plasticizers. During pyrolysis, the degradation of the LDPE began at about 473K (200°C), and the reaction was completed at 723K (450°C). At this temperature, there were release of volatile organic compounds (VOCs) which was detected from the off odor. However, as reported by other researchers, the exact temperature at which LDPE starts to degrade varies depending on various factors such as the grade and additives in the LDPE, the heating rate, and the heating medium (Felgel-Farnholz et al.,2023), Table 3 indicates wax yield relative to the initial weight of the shredded polyethylene (PE) feed to the pyrolysis system at 350°C and 450°C (reference temperatures were chosen based on best temperatures reported by previous studies(Felgel-Farnholz et al.,2023)). The weight loss resulting from the thermal degradation (difference between the initial weight and product weight) must have occurred due to some major breakdown processes during pyrolysis. The sachet water packaging LDPE, a long-chain polymer of ethylene monomers break down in the presence of heat resulting to formation of smaller molecules (Bamps et al.,2023). The chemical reactions responsible for this degradation and wax formation include: random scission, chain unzipping and possibly dehydrogenation (Dai et al.,2022). During this process, chemical bonds along the chain or at the end of the molecule are broken randomly (Mishra et al.,2023), resulting in definite fragmentation into hydrocarbons or formation of shorter hydrocarbon chains (as is the case with chain unzipping). Also, possible removal of hydrogen atoms from the polymer chains which will likely result to formation of unsaturated hydrocarbon. Table 2 shows the effect of temperature on the wax yield. At lesser temperature (350°C) the wax production took more heating time but as temperature increased the wax yield increased from 54.44% to 60.7 and reduction in the heating time from 55min to 35min.

**Table 3: Effect of pyrolysis temperature on the wax yield**

| Pyrolysis Temperature (°C) | Heating time (minutes) | Weight of raw material (g) | Weight of wax produced (g) | Yield (%) |
|----------------------------|------------------------|----------------------------|----------------------------|-----------|
| 450                        | 35                     | 146.628                    | 89.108                     | 60.77     |
| 350                        | 55                     | 40.052                     | 21.776                     | 54.44     |

The same tendencies were also reported by Ullah et al.,2022, where the optimum wax yield from pyrolysis of polyethylene was obtained at a slightly higher temperature (65°C) with a lower operation time. This may be because at higher temperatures, the thermal decomposition of waste materials are faster, resulting to shorter heating times. However, increasing the temperature above 450oC was reported to have negative effect on the wax yield as the volatility of the pyrolysis products tend to increase which can result in loss of yield due to evaporation. Hence, the optimum yield of wax is as a result of the balance between the thermal decomposition rate and the volatility of the gaseous products (Ullah et al.,2022).

### 3.2 Characterization of Polyethylene Wax

A comprehensive characterization of the wax gives valuable insight into the properties and composition of the wax. Furthermore, it can also aid in understanding the potential applications and properties of the LDPE-derived wax for various industrial and commercial purposes (Valizadeh et al.,2024).

**3.2.1 Physical appearance:** The wax obtained was light brown in color and showed glossy appearance. The wax materials were solid at room temperature and relatively brittle. The appearance can be attributed to the pyrolysis condition and resulting changes in the molecular structure during the pyrolysis process (Valizadeh et al.,2024).

**3.2.2 Hardness:** The shore D hardness test results for the two wax samples obtained at 350 and 450 degrees Celsius reported in Table 4 is in agreement with the results reported by previous researchers (Nwapa et al.,2020; Czarnecka-Komorowska; et al.,2020)

Table 4: shore D hardness test response

|                  | 350°C     | 450°C    |
|------------------|-----------|----------|
| Temperature      |           |          |
| Hardness (shore) | 84.33±0.5 | 89.5±0.5 |

A higher shore value indicates a harder wax, which may be preferable in applications that require durability and resistance to deformation. However, a softer wax may be more suitable for applications that require flexibility and malleability. Also, in a case where the wax would be used for coating, it is intended to provide a high gloss finish, then a wax with a higher hardness may be preferred. On the other hand, if the coating is intended to provide better scratch resistance, then a wax with a lower hardness but higher flexibility may be preferred (Wagle et al., 2021). For the production of anti-corrosive coating (TAC-PEW) as undertaken in this study, LDPE-wax of higher hardness was preferred based on the specific need and requirement of durability, wear resistance, scratch resistance, improved barrier properties, among others.

### 3.2.3 Fourier Transform Infrared Spectrometry (FTIR)

FTIR analysis carried out on the polyethylene wax obtained at 350°C and 450°C to study their chemical functional group resulting from the molecular structure adjustment following the pyrolysis process. The results as seen in Figures 4 and 5 are almost similar. The strong and sharp peak was observed at 719.4cm<sup>-1</sup> belonging to CH<sub>2</sub> rocking band. It is attributed to the rocking motion of CH<sub>2</sub> groups within the crystalline regions of the LDPE-wax sample. This peak is a common feature in FTIR spectra of polyethylene-based materials and is particularly prominent in samples with a higher degree of crystallinity. The prominent peak at 1357.4cm<sup>-1</sup> is often associated with the asymmetric bending vibration of CH<sub>3</sub> groups. The presence of this peak indicates the existence of methyl (CH<sub>3</sub>) groups in the LDPE-wax. Methyl groups contribute to the structure of the aliphatic hydrocarbon backbone of the polymers and are common in LDPE-wax. The peak at 1718.3 cm<sup>-1</sup> is commonly associated with the carbonyl (C=O) stretching vibration. The presence of a peak at 1718.3 cm<sup>-1</sup> suggests the existence of carbonyl groups in the LDPE-wax. Carbonyl groups are typically found in compounds such as esters, ketones, aldehydes, and carboxylic acids. Their presence in the FTIR spectrum of LDPE-wax may indicate traces of foreign component or impurities, which may have resulted from the bleaching of the inscription ink from the waste sachet water packaging using nitrocellulose before the pyrolysis.

The presence of this group suggests the need to thoroughly wash the sachets properly after bleaching. The peak at 1461.1 cm<sup>-1</sup> is attributed to the symmetric stretching vibration of CH<sub>2</sub> groups. Like the peak at 719.4 cm<sup>-1</sup>, it indicates the presence of CH<sub>2</sub> groups in the LDPE-wax. The intensity and position of this peak can provide information about the arrangement and interactions of CH<sub>2</sub> groups in the material. The CH<sub>2</sub> group peaks are characteristic of the aliphatic hydrocarbon backbone of LDPE, which is primarily composed of C-C and C-H bonds. The presence of CH<sub>2</sub> groups and the crystalline regions in the LDPE-wax are typical features of the polymer. Also, prominent peaks of intensity 94.5 and 93.7 found at 965.4 and 909.4 cm<sup>-1</sup>, respectively both indicate the presence of CH<sub>2</sub> groups as well and are consistent with the molecular structure of the polymer. LDPE is composed of repeating units of ethylene monomers, and the FTIR spectrum reflects the characteristic vibrational modes of these molecular units (Boronat et al.,2024). Another prominent peak was observed at 1047.4 cm<sup>-1</sup> is likely associated with the asymmetric stretching vibration of C-O-C (carbon-oxygen-carbon) groups. This type of peak strongly suggests the presence of polyethylene glycol (PEG) in the LDPE-wax. PEG is a polymeric compound derived from ethylene glycol and is often used as an additive or plasticizer in various polymer formulations, including LDPE. Hence, this group is expected in LDPE-wax FTIR spectrum. Two others peaks of low intensity were observed at 2914.8cm<sup>-1</sup> and 2847.7cm<sup>-1</sup> are still related to the vibrational modes of CH<sub>2</sub> and CH<sub>3</sub> groups, which are abundant in LDPE (Low-Density Polyethylene) and are part of its aliphatic hydrocarbon backbone.

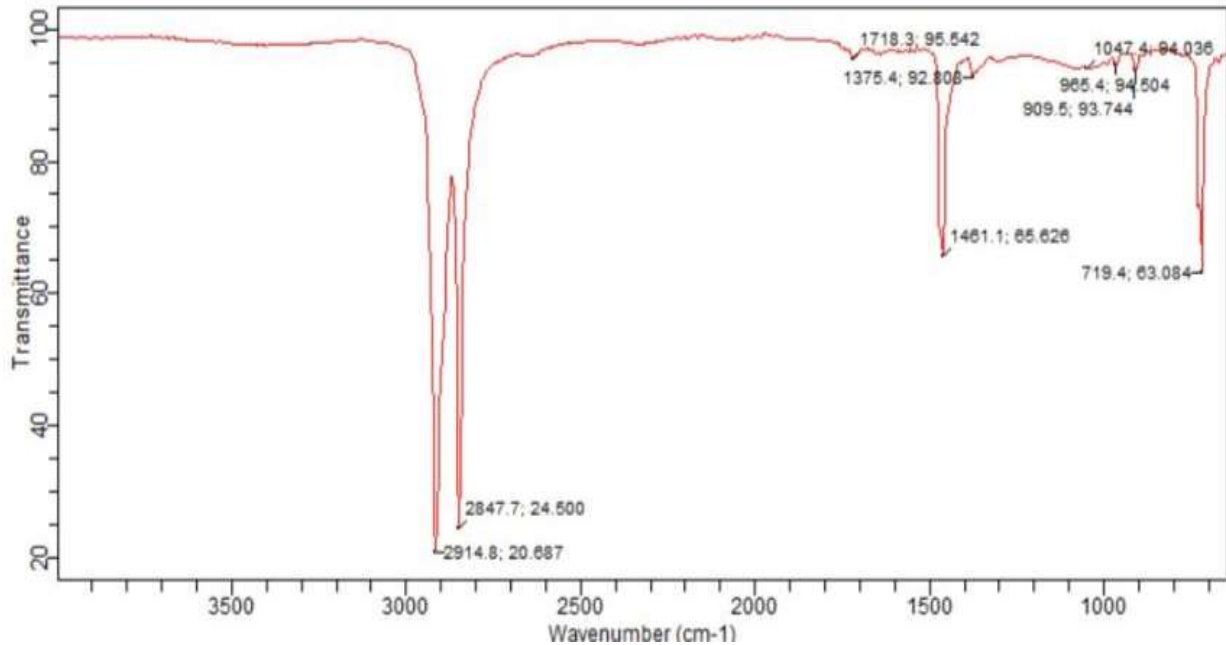


Figure 4: FTIR for wax produced at 450 °C

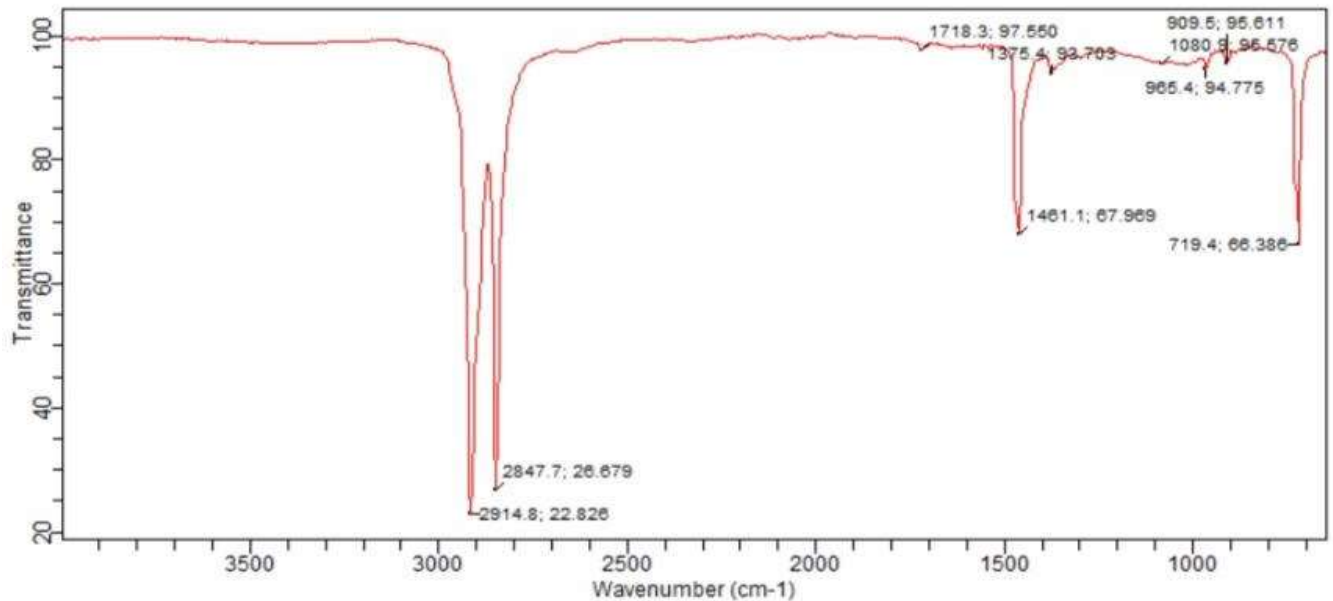
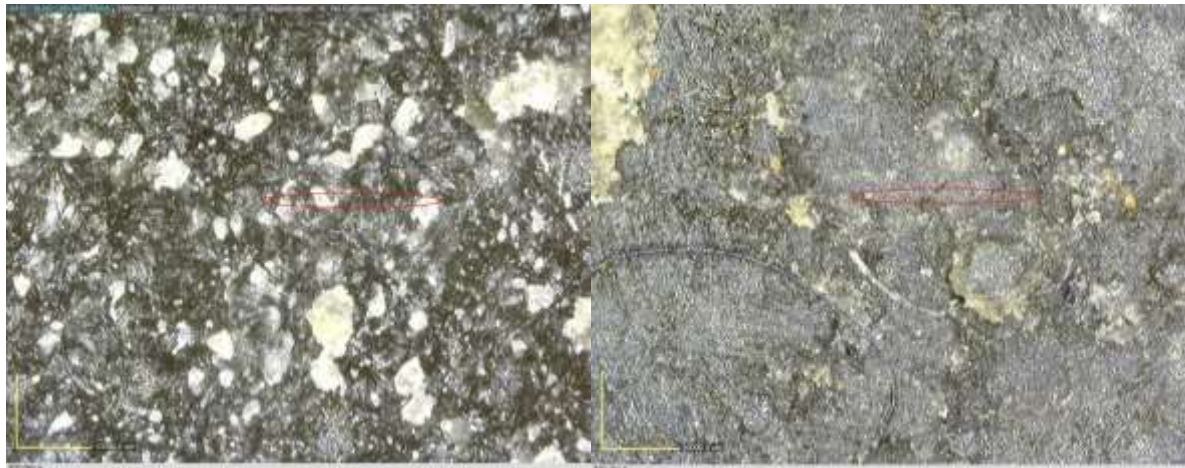


Figure 5: FTIR for wax produced at 350 °C

### 3.3.4 Microscopic examination

The morphological structures of the polyethylene wax obtained at 350°C and 450°C were viewed under microscope. The micrograph analysis of both samples, which presents the optical view of the samples show both the fracture and form surfaces of the wax as seen in Figures 6 and 7. The images reveal that the external surface of the polyethylene obtained at 450°C was very irregular and full of larger cavities with different shapes and sizes compared to that of the polyethylene wax obtained at 350°C. The two surfaces are covered with patches of grey and white. Smaller pores were detected on polyethylene wax obtained at 350°C, whereas large pores were clearly seen on the surface of the polyethylene wax obtained at 450°C. The well-developed pores resulted in larger surface area and more porous structure (Yetgin et al.,2021). Polyethylene wax obtained at 450°C has heterogeneous pore distribution. Higher temperature is believed to be responsible for the pore development in the polyethylene wax obtained at 450°C.



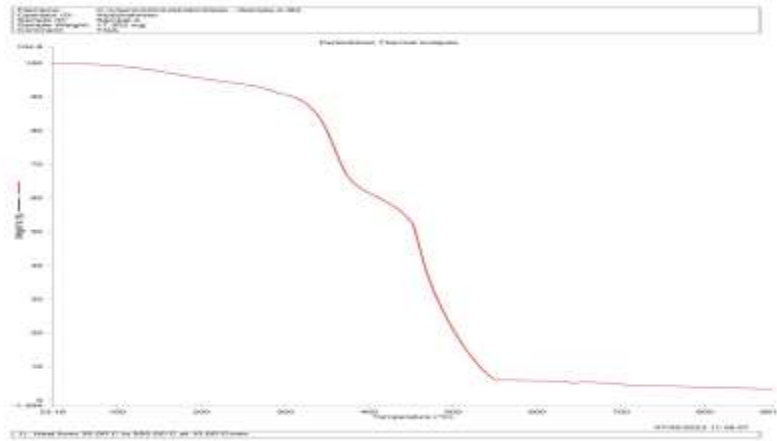
**Figure 6: SEM of wax produced at 450°C a. Fracture form b. Surface form**



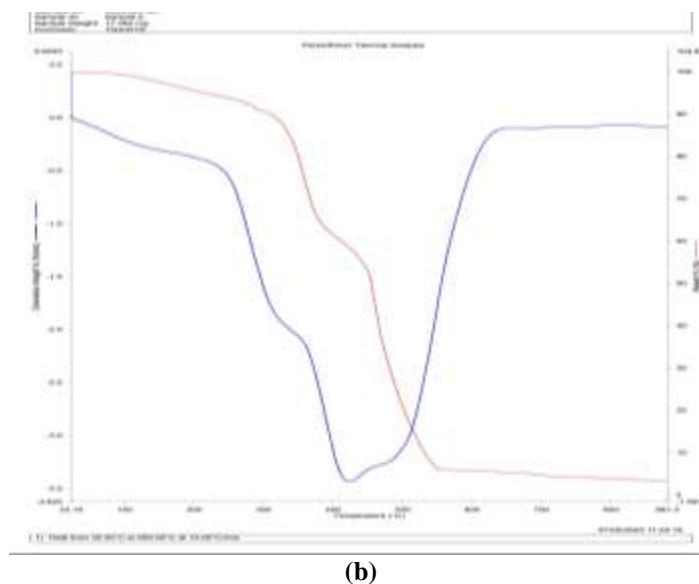
**Figure 7: SEM of wax produced at 350°C a. Fracture form b. Surface form**

**3.3.5 Thermogravimetric Analysis (TGA)**

Thermogravimetric analysis was intended to show the relationship between temperature and mass change of the wax. The expected result will aid the understanding of the mechanism of thermal decomposition.



**(a)**



(b)  
Figure 8: TGA of Wax produced 450°C a. TGA curve b. TGA-DTA curve

The TGA curve in Figure 8a shows the percentage weight loss of the polyethylene wax as a function of increasing temperature. DTA (Differential Thermal Analysis) is a thermal analysis technique used to measure the difference in temperature between the wax sample and a reference material when both are subjected to identical thermal conditions. In this case, the DTA results are combined with the TGA results to produce a TGA-DTA curve as represented in Figure 8b. From the TGA curve, it is seen that there is an initial weight loss of about 0.034% at a temperature of 23.19°C, which may be due to evaporation of any moisture present in the sample. Further increase in temperature, increases the weight loss of the wax, indicating that the wax is undergoing decomposition. The TGA-DTA curve shows that the thermal degradation of the wax took place between 350 and 500°C. Since chemical bonds break more easily at higher temperatures, as temperature rises, a large amount of volatile matter evaporates. The graph shows a broad endothermic peak at around 400-500°C, which may be associated with the decomposition of the wax and indicating a major phase transition or reaction during the heating process. It was found that the wax almost degraded completely, the residue was 3.272% at the final temperature of 881.3°C, which may be attributed to the presence of residual carbon in the sample. From the TGA and DTA results, it could be reported that the polyethylene wax has good thermal stability up to about 500°C, with a gradual weight loss as the temperature increases. This suggests that the wax can be used in high-temperature applications without significant thermal degradation (Yetgin et al.,2021). Based on Fig 8b,

### 3.4 Solvent Selection for TAC-PEW production

The choice of solvent was made between the two most reported mineral solvents: Xylene and isopropyl alcohol (Zolghadr et al.,2021). Preference was based on the virtual consistency of the obtained mixture and the viscosity after dissolution of same quantity of alkyd resin in the solvents. The viscosities of the mixture obtained are presented as Table 5.

**Table 5: Solubility of Alkyd Resin in Xylene and IPA respectively**

| Solvent | Solvent ratio | Alkyd resin ratio | Viscosity (mPa.s) | Consistency/Uniformity |
|---------|---------------|-------------------|-------------------|------------------------|
| IPA     | 1             | 1.5               | 54                | Low                    |
| Xylene  | 1             | 1.5               | 66                | High                   |

For the anti-corrosion coating, solvent that returns a better mixing and high viscosity is needed. Table 5 shows the choice solvent as xylene with viscosity of 66mPa.s and high uniformity. This consistency is due to the fact that alkyd resins have a higher solubility in aromatic solvents such as xylene than in aliphatic solvents or other polar solvent such as Isopropyl alcohol (IPA)(Ifijen et al.,2022. Polar solvents are better suited for dissolving polar

materials. The mixture ratio with xylene also gave a more uniform and consistent mixture with a higher viscosity as seen in Table 5.

### 3.5. Effect of varying major components (titanium dioxide and wax) in preparing TAC-PEW on the corrosion rate of carbon steel

The ratio of titanium-dioxide was varied while other components were kept constant to study the influence of titanium dioxide on reduction of corrosion rate of carbon steel in acidic medium. The TAC-PEW was formulated using the variables ratio in Table 6. The corrosion reduction effect of the TAC-PEW coated on a carbon steel of 1.4 by 1.2 by 0.04 inches immersed in 0.2N of HCL after 4h are shown also in Table 6.

The results in Table 6, shows that increasing the ratio of titanium dioxide in the TAC-PEW formulation resulted in a decrease in weight loss and subsequently decrease in CR of the coated carbon steel samples acidic medium. The trend therefore suggested that the higher the ratio of titanium dioxide, the better the anti-corrosion properties of the coating. This can be attributed to the fact that titanium dioxide is a well-known corrosion inhibitor and has been widely used in anti-corrosion coatings. The increased presence of titanium dioxide in the coating likely provided more corrosion protection to the underlying steel surface, resulting in less weight loss of the samples.

However, there may be an optimal ratio of titanium dioxide in the TAC-PEW formulation beyond which further increases may not lead to significant improvements in anti-corrosion properties, and may even result in decreased coating flexibility; however, that will be reported under variables optimization, which is outside the scope of the present studies.

**Table 6: Effect of varying titanium dioxide weight in formulation of TAC-PEW**

| Ratio         | LDPE-Wax (g) | Alkyd resin (g) (Best ratio) | Xylene (g) (Best ratio) | Titanium dioxide (g) | Cobalt dryer (g) | Weight loss (g) in 0.2N HCl after 4 h | CR(g/m <sup>2</sup> ·h) |
|---------------|--------------|------------------------------|-------------------------|----------------------|------------------|---------------------------------------|-------------------------|
| 1:1.5:1:1:0.2 | 1            | 1.5                          | 1                       | 1                    | 0.2              | 0.32                                  | 19.34                   |
| 1:1.5:1:1:0.2 | 1            | 1.5                          | 1                       | 2                    | 0.2              | 0.23                                  | 13.90                   |
| 1:1.5:1:3:0.2 | 1            | 1.5                          | 1                       | 3                    | 0.2              | 0.19                                  | 11.48                   |

The effect of the LDPE-wax quantity was also studied using 3g of titanium dioxide, other parameters were also held constant at 1.5g of alkyd resin, 1g of solvent and 0.2g of cobalt dryer making a ratio of (x:1.5:1:3:0.2), with x representing the ration for the LDPE-Wax.

**Table 7: Effect of varying titanium dioxide weight in formulation of TAC-PEW**

| Ratio         | Wax (g) | Alkyd resin (g) | Xylene (g) (Best ratio) | Titanium dioxide (g) (Best ratio) | Cobalt Dryer | Weight loss | CR (g/m <sup>2</sup> ·h) |
|---------------|---------|-----------------|-------------------------|-----------------------------------|--------------|-------------|--------------------------|
| 1:1.5:1:3:0.2 | 1       | 1.5             | 1                       | 3                                 | 0.2          | 0.23        | 13.90208                 |
| 2:1.5:1:3:0.2 | 2       | 1.5             | 1                       | 3                                 | 0.2          | 0.22        | 13.29764                 |
| 3:1.5:1:3:0.2 | 3       | 1.5             | 1                       | 3                                 | 0.2          | 0.32        | 19.34202                 |

It can be observed from Table 6, that coating with the 2:1.5:1:3:0.2 wax, alkyd resin, solvent, titanium oxide and cobalt dryer ratio had the least weight loss, while the coating with the 3:1:1:3:0.2 ratio had the highest weight loss. Hence, it shows that increasing the amount of wax in the mixture initially led to a slight increase in the coating's resistance to acid corrosion and finally to a decrease as the weight loss increased. This trend may be due to overloading of the coating with wax which can decrease the availability of active ingredients such as the titanium dioxide and alkyd resin, leading to a reduction in their protective properties (Zolghadr et al.,2021). Also, high wax content can lead to a more brittle coating which makes the coating more susceptible to cracking and exposing the underlying carbon steel to the corrosive medium. Hence, it is always pertinent to optimize the wax quantity for specific applications so that the desired level of corrosion protection would be achieved with the right balance of the active ingredients.

### 3.6 Final TAC-PEW formulation and corrosion inhibition test

The final TAC-PEW formulation was done using for wax, alkyd resin, xylene, titanium dioxide and cobalt dryer ratio of 2:1.5:1:3:0.2 respectively. The result of the rapid corrosion inhibition test carried out using six different steel of each 1.4 by 1.2 by 0.04 inches in 1N of HCl, water and in brine are reported in Table 8. The weight loss recorded in water and brine was relatively insignificant. This must have resulted from the short period of time the steel was exposed to those media. However, the acidic medium provides a harsher environment needed to rapid corrosion test. Furthermore, Table 8 shows the results of the inhibition efficiency (IE) with respect to time. A higher inhibition efficiency percentage indicates that the inhibitor is more effective at suppressing the targeted process. This suggests that the inhibitor is capable of significantly reducing the corrosion impact. The table below show significant inhibition index. The least inhibition efficiency was recorded at 1hr, while the highest was at 5hr with 87.5% inhibition efficiency. This shows that the TAC- PEW coating was effective. The high corrosion efficiency of TAC-PEW can be attributed to the mechanism of the corrosion inhibition of the TAC-PEW components. The titanium dioxide presents in TAC-PEW functions as a barrier and a passivator, preventing the direct contact of the metal surface with acid. Furthermore, Titanium dioxide is amphoteric, it acts as a pH buffer in a corrosive environment, maintaining a more neutral pH at the metal surface. These phenomena can suppress the acidic attack that accelerates corrosion. In addition, the PEW combined with the alkyd resin forms an enhanced adhesion and uniform film formation. This uniformity ensures that the titanium dioxide particles are evenly distributed and provide consistent corrosion inhibition.

PEW are often chemically inert and stable materials ( Zolghadr et al.,2021). Hence, in most cases do not readily react with corrosive substances and is capable of protecting the metal from chemical/acid attack. In an extreme case, the wax due to its inert nature act as a sacrificial layer that undergoes any corrosive attack instead of the underlying metal. It was virtually observed that the coating layer was not depleted during that test time. This is consistent with the combined stability of the alkyd resin, PEW and titanium dioxide. This enhanced stability helped to maintain the TAC-PEW protective barrier's effectiveness under the exposed acidic environmental conditions.

**Table 8: Weight loss of coated carbon steel samples in water, brine and acidic media (initial weight 4.87g)**

| Time (hour) | Control | Control brine | Control acid | Weight loss in water | Weight loss in brine | Weight loss in 1.0N HCl | CR for uncoated Steel (g/m <sup>2</sup> ·h) | CR coated steel (g/m <sup>2</sup> ·h) | IE (%) |
|-------------|---------|---------------|--------------|----------------------|----------------------|-------------------------|---|---------------------------------------|--------|
| 1           | 0.00    | 0.00          | 0.49         | 0.02                 | 0.01                 | 0.20                    | 15.9  | 6.9                                   | 56.51  |
| 2           | 0.00    | 0.00          | 0.77         | 0.01                 | 0.0                  | 0.11                    | 4.38  | 4.2                                   | 81.27  |
| 3           | 0.00    | 0.00          | 0.89         | 0.0                  | 0.02                 | 0.12                    | 3.18  | 0.53                                  | 83.33  |

|   |      |      |      |      |      |      |      |      |       |
|---|------|------|------|------|------|------|------|------|-------|
| 4 | 0.00 | 0.00 | 0.93 | 0.01 | 0.03 | 0.15 | 2.99 | 0.59 | 80.00 |
| 5 | 0.00 | 0.00 | 0.88 | 0.0  | 0.02 | 0.16 | 2.55 | 0.32 | 87.50 |
| 6 | 0.00 | 0.00 | 0.83 | 0.01 | 0.02 | 0.11 | 1.45 | 0.27 | 81.81 |

### 3.7 Kinetics modeling of the corrosion rate data for TAC-PEW in acidic medium

The experimental data from the rapid corrosion test carried out in acidic medium for the un-coated steel, modeled using the kinetic models (Table 1) through sets of python codes (see supplementary materials) yielded kinetic model results as discussed below. Figs 8-10 show the graphical representation of the alignment of the experimental data to the corrosion kinetic models considered. It was observed that the corrosion rate data fitted well with exponential kinetic models much better than other models. Hence, as time (t) increases, the corrosion rate (CR) decreases exponentially. The exponential decay behavior shows that the initial corrosion rate is relatively high, but it decreases rapidly over time. The coefficient of correlation (R<sup>2</sup>) of 0.999 and standard deviation of 4.9 are indications that the model (Equation 15) generated is reliable for further predictions. Collectively, the constants, 'A' and 'B' define the behavior of the corrosion kinetics in the exponential model. The value of 'A' (scaling factor) represents the initial corrosion rate, while the value of 'B' determines how quickly the corrosion rate decreases as time (t) progresses. Hence, A and B can help to quantify the initial corrosion rate and the rate of decay of the corrosion process, providing valuable insights into the corrosion behavior and the effectiveness of corrosion inhibitors or protective measures. The model and experimental scaling factor of 22.97 and 17.78, respectively confirmed that the initial corrosion rate (IE) at time =0 or the decay rate at the beginning of the corrosion process is relatively high. The value of B found to be 0.2529 also indicates rapid decay since the corrosion rates were measured and reported in per hour basis.

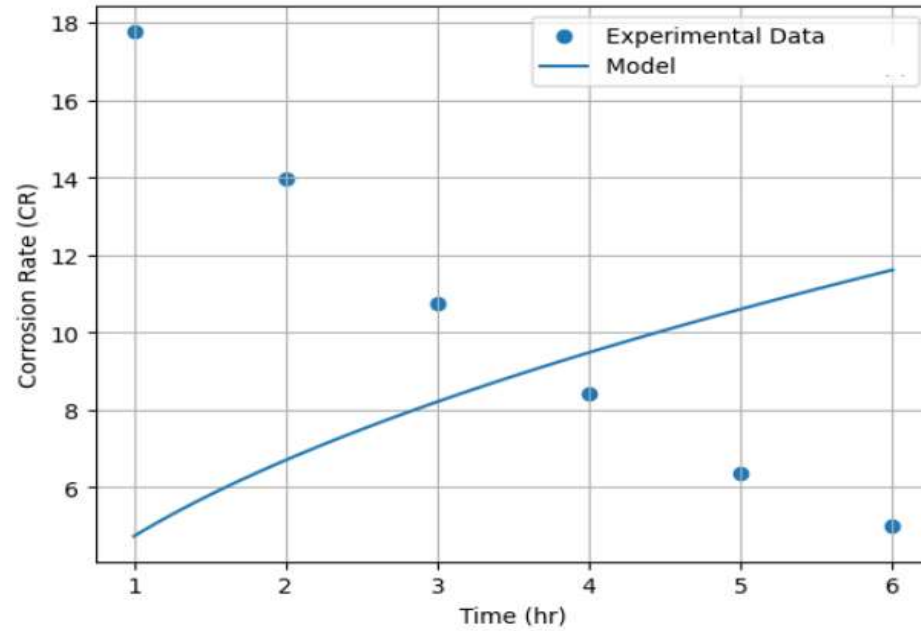
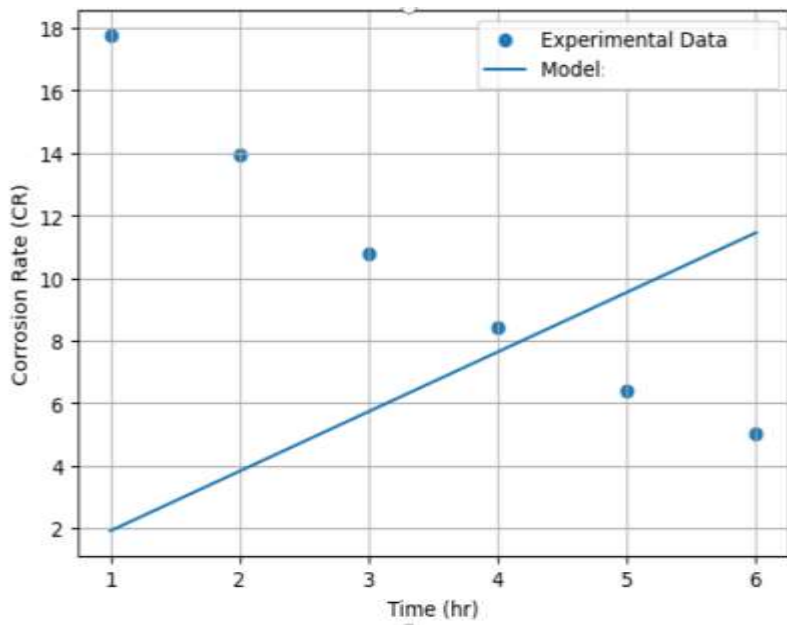


Fig 9 Linear kinetic models

Fig 10 Parabolic kinetic model plot

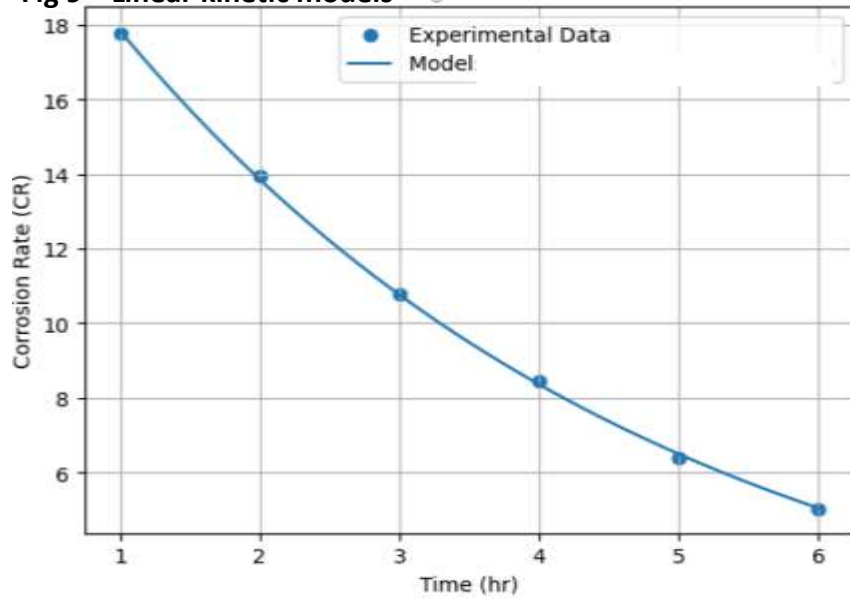


Fig 11 Exponential kinetic model plot

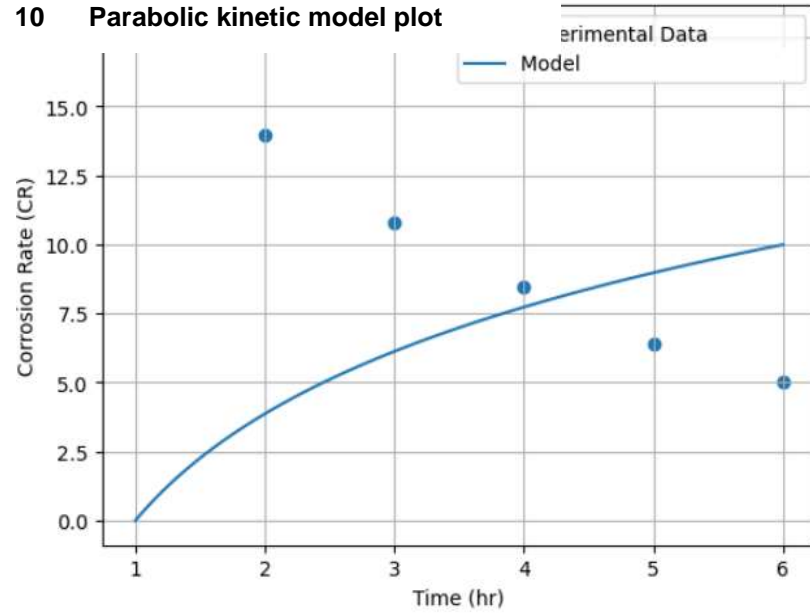


Fig 12 Logarithmic kinetic model plot

**Table 9: Comparison of models predicted CR and experimental CR**

| Time (hr) | Linear Model CR | Parabolic model CR | Exponential model CR | Logarithmic model CR | Experimental CR |
|-----------|-----------------|--------------------|----------------------|----------------------|-----------------|
| 1         | 1.9090          | 4.7417             | 15.53                | 0.0000               | 15.9            |
| 2         | 3.8179          | 6.7058             | 5.43                 | 3.8635               | 4.38            |
| 3         | 5.7269          | 8.2129             | 4.21                 | 6.1234               | 3.18            |
| 4         | 7.6358          | 9.4835             | 3.27                 | 7.7269               | 2.99            |
| 5         | 9.5448          | 10.6029            | 2.54                 | 8.9707               | 2.55            |
| 6         | 11.4538         | 11.6149            | 1.42                 | 9.9869               | 1.45            |

$$CR = 10.4175 * (\exp(-0.2529 * t))$$

15

Based on Equation 15, the extrapolated annual cumulative corrosion of  $41.9 \text{ gm}^{-2} \text{ yr}^{-1}$  and the annual average rate of  $4.70 \times 10^{-3} \text{ gm}^{-2} \text{ h}^{-1}$  were obtained.

### 3.8 Kinetics modeling of the corrosion inhibition efficiency data for TAC-PEW in acidic medium

**Table 10: Comparison of models predicted IE and experimental IE**

| Time (hr) | Linear Model IE | Power Law Model IE | Exponential model IE | Logarithmic model IE | Experimental IE |
|-----------|-----------------|--------------------|----------------------|----------------------|-----------------|
| 1         | 71.8            | 68.20              | 72.53                | 80.64                | 56.51           |
| 2         | 75.3            | 75.64              | 75.60                | 80.64                | 81.27           |
| 3         | 78.8            | 80.36              | 78.80                | 80.64                | 83.33           |
| 4         | 82.4            | 83.90              | 82.14                | 80.64                | 80.00           |
| 5         | 85.9            | 86.74              | 85.61                | 80.64                | 87.50           |
| 6         | 89.5            | 89.14              | 82.23                | 80.64                | 81.81           |

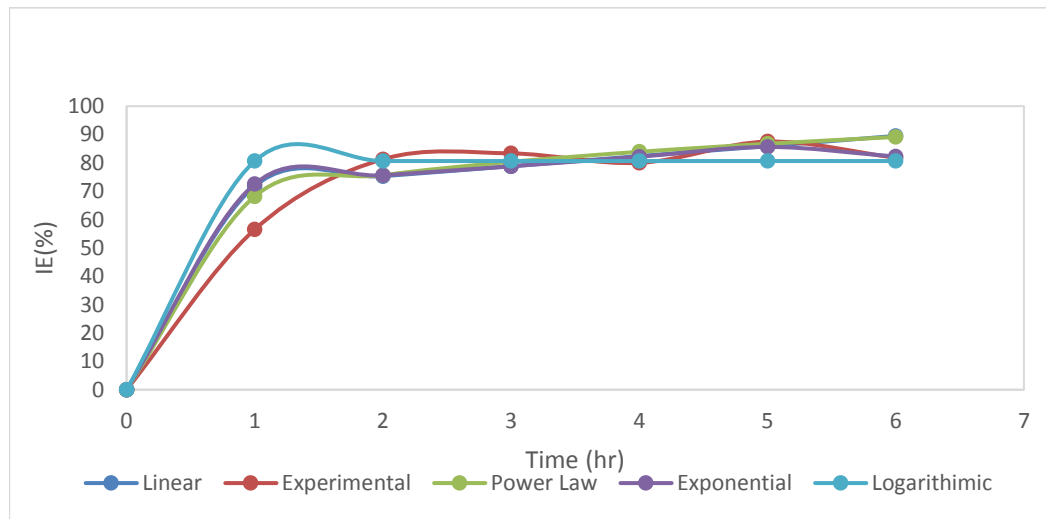


Fig 13: Comparison of experimental and model predicted inhibition efficiency of TAC-PEW coating

Table 11 shows the kinetic models fit with the corrosion rate data. It can be observed that the exponential models excellently described the corrosion rate data. The kinetic studies show the nature of corrosion of the steel in acidic medium without coating with TAC-PEW protective film. The exponential model suggest that the rate of corrosion increases over time exponentially which may be attributed to the breakdown of particles at the surface of the steel as it becomes increasingly reactive with the medium. This can be attributed to formation of corrosion product which in-turns induced further reactions. The magnitude of the exponential model's constant (K - 68.20) showcases the initial dynamics and the acceleration rate of the corrosion process. The K of this magnitude infers very rapid initial corrosion rate which is an indication that the medium was very aggressive. The positive  $\beta$  constant implies that the corrosion rate declines exponentially with time, inferring that the aggressive attack slows down as time progresses. This could be attributed to the fact that corrosion product layer must have been formed on the steel surface which

will provide temporal inhibition or due to the depletion of the corrosive species within the medium. Furthermore, the inhibition efficiency of TAC-PEW coating was evaluated via the study of the inhibition kinetics.

**Table 11: Kinetic models parameters and error functions**

| <b>Corrosion kinetic parameters</b>        |              |              |                      |                      |           |                      |
|--|--------------|--------------|----------------------|----------------------|-----------|----------------------|
| Linear Model                               | <b>K</b>     |              | <b>R<sup>2</sup></b> | <b>SD</b>            |           | <b>X<sup>2</sup></b> |
|  | <b>1.909</b> |              | <b>-0.96</b>         | 4.483363301          |           | 2.03215E-34          |
| Parabolic Rate Model                       | <b>K</b>     |              |                      |                      |           |                      |
|  | <b>4.74</b>  |              | -0.99853             | 3.797642             |           | 0.00011              |
| Exponential Model                          | <b>K</b>     | <b>B</b>     |                      |                      |           |                      |
|  | <b>68.20</b> | <b>0.25</b>  | 0.999855             | 4.590512             |           | 1                    |
| Logarithmic Model                          | <b>K</b>     |              |                      |                      |           |                      |
|  | <b>5.57</b>  |              | <b>0.7</b>           | <b>5.6343</b>        |           | <b>0.231</b>         |
| <b>Inhibition Kinetic model Parameters</b> |              |              |                      |                      |           |                      |
| Parameters                                 | <b>a</b>     | <b>B</b>     | <b>c</b>             | <b>R<sup>2</sup></b> | <b>SD</b> | <b>X<sup>2</sup></b> |
| Linear                                     | <b>19.02</b> | 3.53         | -                    | 0.61601              | 8.469693  | 0.420794             |
| Exponential model                          | <b>69.59</b> | <b>-0.04</b> | -                    | 0.930591             | 10.77312  | 0.916929             |
| The logistic model                         | 80.64        | 38.00        | -78.66               | 0.8                  | 38.80356  | 0.215796             |
| Power Law Model                            | 68.20        | 0.15         | -                    | 0.748767             | 8.891774  | 0.646348             |

The TAC-PEW inhibition data in Table 11 shows the least inhibition efficiency (IE) of 59.18% at 1hr and the highest efficiency of 86.75% at the 5<sup>th</sup> hour. This infers that TAC-PEW provides excellent inhibition against corrosion of the steel. The highly significant initial inhibition efficiency and the subsequent rapid increase in rate after the initial suggests that there was a strong interaction between steel surface and TAC-PEW producing a robust barrier against the corrosive agents. Furthermore, it was observed that the overall efficiency was consistently high, which infers that the coating can sustain its protective ability on the steel over an extended period. Slight but continuous variation or fluctuations after the initial inhibition efficiency may be attributed to either environmental factor, partial degradation of coating or surface dynamics. The inhibition efficiency data followed exponential model as well, this can be seen virtually from Fig 13, with strong correlation coefficient (R<sup>2</sup> value) in Table 11. The exponential model constant a and b were found to be 69.59 and 0.04 respectively. The constant “a” being theoretical inhibition efficiency supports the claim of strong interaction between the TAC-PEW and the steel surface, while low “b”, show the rate at which inhibition efficiency decreases over time. Hence low “b” as obtained is desirable. It shows that the strength of TAC-PEW in protecting the steel surface does not deplete rapidly.

#### 4.0 Conclusion

This work successfully created and tested a titanium-based anti-corrosion polyethylene wax (TAC-PEW) coating made from waste LDPE water sachets. The coating displayed good corrosion inhibition efficacy in acidic environments, with a peak value of 86.7%, as validated by robust kinetic modeling in Python. The exponential decrease of corrosion rate and inhibition efficiency demonstrates TAC-PEW's long-term effectiveness in safeguarding carbon steel. This approach solves key environmental and industrial corrosion control challenges by recycling waste materials into high-performance coatings. The findings serve as a solid platform for further optimization and large-scale TAC-PEW applications in a variety of industries.

**Acknowledgment:** The authors express their gratitude to TETFUND Nigeria for their support. The research was sponsored under “ 2024 TetFund intervention in research(RP) Batch 18, No 8.

#### References

Al-Amiery, A., Isahak, W. N. R. W., & Al-Azzawi, W. K. 2024. Sustainable corrosion Inhibitors: A key step towards environmentally responsible corrosion control. *Ain Shams Engineering Journal*, 102672.

- Aljibori, H. S., Alamiery, A., & Kadhum, A. A. H. 2023. Advances in corrosion protection coatings: A comprehensive review. *Int. J. Corros. Scale Inhib*, 12(4), 1476-1520.
- Aljibori, H., Al-Amiery, A., & Isahak, W. N. R. 2024. Advancements in corrosion prevention techniques. *Journal of Bio-and Tribo-Corrosion*, 10(4), 78.
- Bamps, B., Buntinx, M., & Peeters, R. 2023. Seal materials in flexible plastic food packaging: A review. *Packaging Technology and Science*, 36(7), 507-532.
- Boronat, C., Correcher, V., Benavente, J. F., & Bravo-Yagüe, J. C. 2024. Thermoluminescence and ATR-FTIR study of UVC-irradiated low-density polyethylene (LDPE) food packaging. *Spectrochimica Acta Part A: Molecular and Biomolecular Spectroscopy*, 323, 124882.
- Castillo-Robles, J. M., de Freitas Martins, E., Ordejón, P., & Cole, I. 2024. Molecular modeling applied to corrosion inhibition: a critical review. *npj Materials Degradation*, 8(1), 72.
- Czarnecka-Komorowska, D., Grześkowiak, K., Popielarski, P., Barczewski, M., Gawdzińska, K., & Popławski, M. 2020. Polyethylene wax modified by organoclay bentonite used in the lost-wax casting process: processing– structure– property relationships. *Materials*, 13(10), 2255.
- Dai, L., Zhou, N., Lv, Y., Cheng, Y., Wang, Y., Liu, Y., ... & Ruan, R. 2022. Pyrolysis technology for plastic waste recycling: A state-of-the-art review. *Progress in Energy and Combustion Science*, 93, 101021.
- Dubdub, I., & Al-Yaari, M. 2020. Pyrolysis of low density polyethylene: kinetic study using TGA data and ANN prediction. *Polymers*, 12(4), 891.
- Enikeev, M. R., Potemkin, D. I., Enikeeva, L. V., Enikeev, A. R., Maleeva, M. A., Snytnikov, P. V., & Gubaydullin, I. M. 2020. Analysis of corrosion processes kinetics on the surface of metals. *Chemical Engineering Journal*, 383, 123131
- Felgel-Farnholz, A., Schweighuber, A., Klampfl, C. W., & Fischer, J. 2023 Comparative study on the degradation of HDPE, LLDPE and LDPE during multiple extrusions. *Polymer Degradation and Stability*, 216, 110486.
- Ifijen, I. H., Maliki, M., Odiachi, I. J., Aghedo, O. N., & Ohiocheoya, E. B. 2022. Review on solvents based alkyd resins and water borne alkyd resins: impacts of modification on their coating properties. *Chemistry Africa*, 5(2), 211-225.
- Jia, H., Qiao, G., & Han, P. 2022. Machine learning algorithms in the environmental corrosion evaluation of reinforced concrete structures-A review. *Cement*
- Mishra, R., Kumar, A., Singh, E., & Kumar, S. 2023. Recent research advancements in catalytic pyrolysis of plastic waste. *ACS Sustainable Chemistry & Engineering*, 11(6), 2033-2049.
- Nwapa, C., Okunwaye, O. J., Okonkwo, C. L., & Chimezie, O. W. 2020. Mechanical properties of high density polyethylene and linear low density polyethylene blend. *SSRG International Journal of Polymer and Textile Engineering (SSRG-IJPTE)*, 7, 22-28.
- Raschka, S., Patterson, J., & Nolet, C. 2020. Machine learning in python: Main developments and technology trends in data science, machine learning, and artificial intelligence. *Information*, 11(4), 193.
- Shwetha, K. M., Praveen, B. M., & Devendra, B. K. 2024. A review on corrosion inhibitors: types, mechanisms, electrochemical analysis, corrosion rate and efficiency of corrosion inhibitors on mild steel in an acidic environment. *Results in Surfaces and Interfaces*, 100258.
- Thomas, D., Philip, E., Sindhu, R., Ulaeto, S. B., Pugazhendhi, A., & Awasthi, M. K. 2022. Developments in smart organic coatings for anticorrosion applications: a review. *Biomass Conversion and Biorefinery*, 12(10), 4683-4699.
- Tian, Z., Fu, C., & Ye, H. 2024. Mechanisms and kinetic model for steel corrosion in unsaturated cementitious materials. *npj Materials Degradation*, 8(1), 20.
- Ullah, F., Zhang, L., Ji, G., Irfan, M., Ma, D., & Li, A. 2022. Experimental analysis on products distribution and characterization of medical waste pyrolysis with a focus on liquid yield quantity and quality. *Science of the Total Environment*, 829, 154692.
- Valizadeh, S., Valizadeh, B., Seo, M. W., Choi, Y. J., Lee, J., Chen, W. H., ... & Park, Y. K. 2024. Recent advances in liquid fuel production from plastic waste via pyrolysis: Emphasis on polyolefins and polystyrene. *Environmental Research*, 118154.
- Wagle, P. G., Tamboli, S. S., & More, A. P. 2021. Peelable coatings: A review. *Progress in Organic Coatings*, 150, 106005.
- Yetgin, S., Gonen, M., Savrik, S. A., & Balkose, D. 2021. Polyethylene Wax: Uses, Characterization, and Identification. In *Imidic Polymers and Green Polymer Chemistry* (pp. 265-284). Apple Academic Press.
- Zolghadr, A., Foroozandehfar, A., Kulas, D. G., & Shonnard, D. 2021. Study of the viscosity and thermal characteristics of polyolefins/solvent mixtures: applications for plastic pyrolysis. *ACS omega*, 6(48), 32832-32840.